The Accuracy of Rotational Parameters Predicted by High-level Quantum-Chemical Calculations: The Case Study of Sulfur-Containing Molecules of Astrochemical Interest

Silvia Alessandrini,[†,¶] Jürgen Gauss,[‡] and Cristina Puzzarini[*,†]

Dipartimento di Chimica "Giacomo Ciamician", Università di Bologna, Via F. Selmi 2, I-40126 Bologna, Italy, and Institut für Physikalische Chemie, Johannes Gutenberg-Universität Mainz, D-55099 Mainz, Germany

E-mail: cristina.puzzarini@unibo.it

[*]To whom correspondence should be addressed
[†]Università di Bologna
[‡]Johannes Gutenberg-Universität Mainz
[¶]Present address: Scuola Normale Superiore, Piazza dei Cavalieri 7, I-56126 Pisa, Italy

Abstract

The accuracy of rotational parameters obtained from high-level quantum-chemical calculations is discussed for molecules containing second-row atoms. The main focus is on computed rotational constants for which two statistical analyses have been carried out. A first benchmark study concerns sulfur-bearing species and involves 15 molecules (for a total of 74 isotopologues). By comparing 15 different computational approaches, all of them based on the coupled-cluster singles and doubles approach (CCSD) augmented by a perturbative treatment of triple excitations, CCSD(T), we have analysed the effects on computed rotational constants due to: (*i*) extrapolation to complete basis-set limit, (*ii*) correlation of core electrons, and (*iii*) vibrational corrections to rotational constants. To extend the analysis to other molecules containing second-row elements, as well as to understand the effect of higher excitations, a second benchmark study involving 11 molecules (for a total of 54 isotopologues) has been performed. Finally, the rotational parameters of seven sulfur-containing molecules of astrochemical interest (CCS, C_3S, C_4S, C_5S, $HCCS^+$, HC_4S^+ and $HOCS^+/HSCO^+$) have been computed and compared to experimental data, when available, also addressing the direct comparison of simulated and experimental rotational spectra.

1 Introduction

Rotational spectroscopy plays a crucial role in astrochemical and astrophysical studies because molecular species in the interstellar medium (ISM) are in most cases detected via their rotational signatures.[1,2] Indeed, the observation of spectroscopic signatures provides the unequivocal proof of the presence of the chemical species of interest,[3] which in turn is the starting point for the development of astrochemical models. To this end, the rotational spectra of molecules of astrophysical and -chemical interest are investigated in laboratory studies: rotational transitions are recorded in extended frequency regions and then analysed and assigned. The derived spectroscopic parameters are used to predict rotational transitions that have not been directly measured; therefore, the accuracy and reliability of these constants are of great importance. In fact, the detection of a molecular species in space by rotational spectroscopy critically depends on the availability of accurate predictions of rotational transitions and in turn of the corresponding spectroscopic parameters. Among them the rotational constants are the most important ones.[4] Nowadays, the availability of large instantaneous bandwidth receivers, which are also characterized by high spectral resolution, allows for large spectral surveys with uniform sensitivity. These surveys are clearly the ideal means to obtain a complete census of the species that emit in the recorded spectral survey. However, the simultaneous presence of the spectroscopic features of several molecules requires the rotational transition frequencies to be known with an accuracy of a few hundreds of kHz or even better.

To guide the first steps of the spectral assignment procedure in laboratory, as well as to verify the reliability of rotational spectroscopic parameters determined from experiments, quantum-chemical calculations are increasingly employed (see, for example, refs. 5–7). To support the experimental investigation computational predictions of rotational spectra should be accurate, thus implying that high-level quantum-chemical calculations are to be used. These predictions involve two tasks, namely (a) the determination of the required spectroscopic parameters, and (b) the simulation of the spectra based on the given

set of spectroscopic parameters. The latter typically involves the diagonalization of an appropriate Hamiltonian, while the accurate determination of the spectroscopic parameters requires a quantum-chemical treatment of the molecular system under consideration. In the last decade, numerous theoretical studies reporting computed rotational constants have been published (see, for example, refs. 5,6,8 and 9). However, a systematic investigation of the accuracy achievable in quantum-chemical computations of these parameters has been carried out for most parts only for molecular species containing first-row elements.[8]

There is a great astrophysical interest in S-containing molecules because, despite the fact that simple diatomic species up to astronomical complex molecules such as ethyl mercaptan (CH_3CH_2SH) have been detected in interstellar gas clouds and circumstellar outflows (see, for example, refs. 10,11), the details on the sulfur chemistry that takes place in space are mostly unknown. Indeed, while sulfur compounds in the gas phase have been observed in the diffuse ISM with almost no depletion with respect to its solar abundance,[12] the sulfur abundances detected in the cold and dense ISM are much lower.[13] This is known as the "sulfur exhaustion problem"[14] with the chemical form of the missing sulfur not yet being identified. For this reason, there is a great interest in the spectroscopic characterization of neutral as well as ionic sulfur-containing species.

The quantum-chemical approaches employed throughout our calculations are based on coupled-cluster techniques.[15] To investigate their accuracy two systematic benchmark studies have been carried out. The first one focuses on the rotational constants of S-bearing species (with 15 different molecules and 74 isotopologues being considered). Starting from the coupled-cluster singles and doubles approach (CCSD) augmented by a perturbative treatment of triple excitations, CCSD(T),[16] in conjunction with a polarized triple-zeta quality basis set, computational approaches which differ in the treatment of core-correlation and in the extrapolation to the basis-set limit have been considered. To extend our analysis as well as to understand the effect of higher-order excitations, a second benchmark investigation involving molecules containing different second-row elements,

namely S, P, S and Cl (with 11 molecules and 54 isotopologues being considered), has also been performed.

The present investigation is intended to provide a statistical analysis for rotational constants of molecules containing second-row elements, with a particular focus on sulfur-bearing species. The computational methodologies employed in the benchmark studies have also been applied to sulfur-containing molecules of strong astrochemical interest, thus providing an accurate spectroscopic characterization of the thiocumulenes family C_nS, with n=2, 3, 4 and 5, and of the protonated species $HCCS^+$, HC_4S^+, and $HSCO^+/HOCS^+$. While for the neutral molecules some experimental data are available, these are completely lacking for the cations, thus preventing so far the possibility of their detection in space. Therefore, for the C_nS family the main aim is to complement the experiment, while for the cationic species the present work provides the first accurate computational spectroscopic characterization. The paper is organized as follows. In the succeeding section computational details are described with particular emphasis on the calculations of the spectroscopic parameters of interest and the benchmark studies. In the subsequent section, the results of the two benchmark studies are reported and discussed. Finally, the accuracy obtained for two different categories of species, small- and medium-sized molecules, of astrochemical interest are presented and discussed.

2 Computational details

In the present study, quantum-chemical calculations are based on the coupled-cluster (CC) theory[15] for the treatment of the electron correlation and have been performed using the hierarchic series of correlation consistent basis sets developed by Dunning and collaborators.[17–19] For open-shell species, the unrestricted-HF reference wavefunction has been employed. The quantum-chemical package CFOUR[20] has been used throughout,with the only exception of the CC singles, doubles and triples, CCSDT,[21,22] and CC with singles, doubles, triples, quadruples, CCSDTQ,[23] calculations which have been carried out using the general CC program MRCC by Kállay[24] interfaced to the CFOUR package.

2.1 Spectroscopic parameters

The theoretical background of the spectroscopic parameters needed for the accurate simulation of the rotational spectrum are briefly reviewed in the following subsections. The focus is mainly on the computational tasks these parameters require for their determination.

Rotational constants

Rotational constants are the main parameters that determine the rotational spectrum. Molecules can have up to three different rotational constants ($A \geq B \geq C$) corresponding to the three inertial axis (a, b, and c). In our case, those of interest are the rotational constants for the vibrational ground-state, generally denoted as B_0^i, with i indicating an inertial axis.

The vibrational ground state rotational constants can be decomposed as:

$$B_0^i = B_e^i + \Delta B_0^i \,, \tag{1}$$

where B_e^i is the equilibrium rotational constant, i.e., the one that corresponds to the minimum of the Born-Oppenheimer (BO) potential energy surface (PES), while ΔB_0^i represents its vibrational correction.

The equilibrium contribution depends only on the isotopic composition of the molecule and on its equilibrium structure r_e. Consequently, B_e^i is obtained in a straightforward manner from a geometry optimization. By means of second-order vibrational perturbation theory (VPT2),[25] the vibrational correction can be expressed as:

$$\Delta B_0^i = -\sum_r \alpha_r^i \left(v_r + \frac{1}{2} \right) , \tag{2}$$

where the sum runs over all normal coordinates (r) with v_r as the corresponding vibrational quantum number. The α_r^i in eq. (2) are the vibration-rotation interaction constants.[5] To evaluate the ΔB_0^i term, an anharmonic force field has to be computed. The reader is referred to refs. 26–29 for a detailed description on how this task can be accomplished.

Since B_e^i provides by far the largest contribution to B_0^i, high accuracy is required for its determination. This can be achieved by means of composite approaches, with the latter permitting to evaluate various contributions separately, each at the highest possible level of theory, and to combine them together using the additivity scheme.[8,30,31] The contributions that are combined are obtained in the following manner:

1. Extrapolation to the complete basis-set (CBS) limit of the Hartree-Fock energy using the exponential three-point formula by Feller[32] in conjunction with either the cc-pVQZ, cc-pV5Z, and cc-pV6Z basis sets (option 1) or the cc-pVTZ, cc-pVQZ, and cc-pV5Z basis sets (option 2).

2. Extrapolation to the CBS limit of the CCSD(T) correlation energy, evaluated within the frozen-core (fc-) approximation using the two-point equation reported in refs. 33,34. The basis sets used in combination with 'option 1' denoted above are either cc-pVQZ and cc-pV5Z or cc-pV5Z and cc-pV6Z, while for 'option 2', cc-pVTZ and cc-pVQZ have been used.

   This contribution, together with the previous one, is referred to as: fc-CCSD(T)/CBS(Q,5) for 'option 1a', fc-CCSD(T)/CBS(5,6) for 'option 1b', and fc-CCSD(T)/CBS(T,Q)

for 'option 2'.

3. The core-correlation contribution: This term is obtained as the difference between all-electron and fc-CCSD(T) calculations using the same basis set, either cc-pCVQZ or cc-pCVTZ.[35,36]

   The contribution is referred to as core/cc-pCVQZ or core/cc-pCVTZ, respectively..

4. Full treatment of triple excitations beyond CCSD(T). This correction is obtained as the energy difference between the CCSDT and CCSD(T) levels of theory using the cc-pVTZ basis set.

   The contribution is referred to as ΔT.

5. Full treatment of the quadruple excitations, which is obtained as the energy difference between CCSDTQ and CCSDT. Due to its high computational cost, this contribution is computed using a small basis set, cc-pVDZ.

   This contribution is referred to as ΔQ.

By combining all of these contributions, different composite schemes can be defined, with the fc-CCSD(T)/CBS(5,6) + core/cc-pCVQZ + ΔT + ΔQ one being the theoretically most complete and thus the best one. It is noted that the extrapolation schemes above were originally developed for energies; however, their use for forces (gradients)[8,30,31] can be justified because the corrisponding geometry optimization provides the minima on the extrapolated potential-energy surface.

The B_0^i's have then been obtained by adding vibrational corrections to the equilibrium rotational constants, as indicated in equation (1). These corrections have been obtained from a cubic force field computed at either the CCSD(T)/cc-pCVQZ or fc-CCSD(T)/cc-pVTZ level of theory. According to the detailed analysis of errors carried out in ref. 37, the two levels of theory considered should provide accurate estimates for vibrational corrections.

Centrifugal-Distortion Constants

When aiming at high accuracy in the prediction of spectra, additional rotational parameters need to be considered. In particular, the quartic and sextic centrifugal-distortion constants have a non negligible effect on the actual frequencies of rotational transitions. The quartic centrifugal-distortion constants (D, d) require the evaluation of a harmonic force field, while the sextic constants (H, h) necessitate the computation of a cubic force field. The levels of theory considered in the present work for these constants are fc-CCSD(T)/cc-pVTZ, fc-CCSD(T)/cc-pVQZ, and CCSD(T)/cc-pCVQZ.

Electron Spin-Rotation Constant

In the case of open-shell molecules, a coupling between the magnetic moment associated to the spin of the unpaired electrons and the magnetic field generated by the rotation motion occurs. This interaction is described by the electron spin-rotation coupling constant, denoted as γ. The latter is calculated in a perturbative manner as second derivative of the energy with respect to the electron spin and the rotational angular momentum as perturbations, as described in Ref. 38. For the calculations presented in the following, the CCSD method has been used in conjunction either with the aug-cc-pCVQZ basis set[19,39] or, within the frozen-core approximation together with the aug-cc-pVTZ set.

2.2 Benchmark study

Based on the fact that theoretical predictions are based on approximate quantum-chemical schemes, a proper estimate of the corresponding uncertainty is needed. Numerous studies on the accuracy of computed molecular properties and energies,[40–42] geometrical parameters,[30,31,43–45] and spectroscopic quantities[5,8] have been reported in the literature. However, a lack of reliable statistics for systems containing second-row atoms is noted in the case of rotational constants. To fill this gap, the results of two benchmark studies are reported in

the following.

To analyze the rotational parameters obtained from the different schemes, statistical measures are used. This means that for each computational approach we report the mean error ($\bar{\Delta}$), the mean absolute error ($\bar{\Delta}_{abs}$), the maximum error (Δ_{max}), and the standard deviation (Δ_{std}). By denoting as Δ_k the deviation of the computed value from its corresponding experimental counterpart, these statistical measures are defined as:

$$\bar{\Delta} = \frac{1}{n}\sum_{k=1}^{n}\Delta_k \,, \tag{3}$$

$$\bar{\Delta}_{abs} = \frac{1}{n}\sum_{k=1}^{n}|\Delta_k| \,, \tag{4}$$

$$\Delta_{max} = \max_k |\Delta_k| \,, \tag{5}$$

$$\Delta_{std} = \sqrt{\frac{1}{n-1}\sum_{k=1}^{n}(\Delta_k - \bar{\Delta})^2} \,, \tag{6}$$

with the sums running over the n available values. All experimental rotational constants are considered with the same statistical weight in the analysis. This means that for linear molecules the weight of the unique rotational constant is 3, while for the asymmetric tops the weight of each rotational constant is 1.

Assuming that the errors follow a normal distribution, a pictorial representation of our results for each computational approach is obtained via:

$$\rho(\Delta) = \frac{1}{\sqrt{2\pi}\Delta_{std}}\exp\left[-\frac{1}{2}\left(\frac{\Delta-\bar{\Delta}}{\Delta_{std}}\right)^2\right] \,, \tag{7}$$

where $\frac{1}{\sqrt{2\pi}\Delta_{std}}$ is a normalization constant.

Benchmark I

The first benchmark focuses on the rotational constants of S-bearing species and the results for 15 different computational approaches have been compared.

We start with the following levels of theory:

1. fc-CCSD(T)/cc-pVTZ
2. fc-CCSD(T)/cc-pVQZ
3. fc-CCSD(T)/cc-pV5Z

To evaluate the effect of core correlation we continue with the following schemes:

4. CCSD(T)/cc-pCVQZ
5. fc-CCSD(T)/cc-pV5Z + core/cc-pCVTZ

where the former stands for all-electron calculations at the CCSD(T) level using cc-pCVQZ. The second approach instead use an additivity scheme and considers the core-correlation contribution obtained at the CCSD(T)/cc-pCVTZ level on top a fc-CCSD(T)/cc-pV5Z calculation.
To estimate the CBS limit, the extrapolation formula previously mentioned have been used. We consider here:

6. fc-CCSD(T)/CBS(T,Q)
7. fc-CCSD(T)/CBS(Q,5)

i.e., two schemes that have been already introduced in section 2.1.
Using the additivity schemes, core correlation can also be considered for the last two approaches. Both the cc-pCVTZ and cc-pCVQZ basis sets have been employed, thus yielding to four different composite schemes:

8. fc-CCSD(T)/CBS(T,Q) + core/cc-pCVTZ
9. fc-CCSD(T)/CBS(T,Q) + core/cc-pCVQZ
10. fc-CCSD(T)/CBS(Q,5) + core/cc-pCVTZ

11. fc-CCSD(T)/CBS(Q,5) + core/cc-pCVQZ

The equilibrium rotational constants obtained within the last four approaches have then been corrected for vibrational corrections, ΔB_0^i, to obtain the B_0^i constants. These corrections have been obtained at the fc-CCSD(T)/cc-pVTZ level. This leads to the following four schemes:

12. fc-CCSD(T)/CBS(T,Q) + core/cc-pCVTZ + ΔB_0^i/cc-pVTZ

13. fc-CCSD(T)/CBS(T,Q) + core/cc-pCVQZ + ΔB_0^i/cc-pVTZ

14. fc-CCSD(T)/CBS(Q,5) + core/cc-pCVTZ + ΔB_0^i/cc-pVTZ

15. fc-CCSD(T)/CBS(Q,5) + core/cc-pCVQZ + ΔB_0^i/cc-pVTZ

All computational approaches have been applied to 9 closed- and 6 open-shell molecules, and in this way a total of 74 isotopologues were considered in our first benchmark (see Table I).

Benchmark II

To extend the analysis to other molecules containing second-row elements as well as to investigate the effect of higher excitations, a second benchmark investigation has been carried out using a set of 11 small molecules (and a total of 54 isotopologues) containing other second-row elements: HCl, SiS, PN, CS, OCS, H_2S, HBS, FBS, HCP, FCP, and ClCP. The complete list of isotopologues considered in this benchmark is given in Table II.

For this study, seven levels of theory have been considered:

1. fc-CCSD(T)/CBS(5,6)

2. fc-CCSD(T)/CBS(5,6) + core/cc-pCVQZ

3. fc-CCSD(T)/CBS(5,6) + core/cc-pCVQZ + ΔT

Table I: List of molecules and isotopic species employed in the "benchmark I" study.

Molecule	Isotopologues
CS	$^{12}C^{32}S$, $^{12}C^{34}S$, $^{12}C^{33}S$, $^{12}C^{36}S$
	$^{13}C^{32}S$, $^{13}C^{33}S$, $^{13}C^{34}S$
CS^+	$^{12}C^{32}S^+$
CCS	$^{12}C^{12}C^{32}S$, $^{12}C^{12}C^{34}S$
C_3S	$^{12}C^{12}C^{12}C^{32}S$, $^{12}C^{12}C^{12}C^{34}S$, $^{13}C^{12}C^{12}C^{32}S$
	$^{12}C^{13}C^{12}C^{32}S$, $^{12}C^{12}C^{13}C^{32}S$, $^{13}C^{12}C^{12}C^{34}S$
	$^{12}C^{13}C^{12}C^{34}S$, $^{12}C^{12}C^{13}C^{34}S$, $^{13}C^{12}C^{13}C^{32}S$
	$^{12}C^{13}C^{13}C^{32}S$
C_3O	$^{12}C^{12}C^{12}C^{16}O$, $^{12}C^{12}C^{12}C^{18}O$, $^{13}C^{12}C^{12}C^{16}O$
	$^{12}C^{13}C^{12}C^{16}O$, $^{12}C^{12}C^{13}C^{16}O$
HCS	$D^{12}C^{32}S$
HSC	$H^{32}S^{12}C$, $D^{32}S^{12}C$
HCS^+	$H^{12}C^{32}S^+$, $D^{12}C^{32}S^+$, $H^{13}C^{32}S^+$, $H^{12}C^{34}S^+$
SO	$^{32}S^{16}O$, $^{34}S^{16}O$, $^{32}S^{17}O$, $^{32}S^{18}O$
SO_2	$^{32}S^{16}O^{16}O$, $^{33}S^{16}O^{16}O$, $^{34}S^{16}O^{16}O$, $^{32}S^{17}O^{16}O$
	$^{32}S^{18}O^{16}O$
HSO	$H^{32}S^{16}O$, $D^{32}S^{16}O$
OCS	$^{16}O^{12}C^{32}S$, $^{16}O^{13}C^{32}S$, $^{17}O^{12}C^{32}S$, $^{16}O^{12}C^{34}S$
	$^{16}O^{12}C^{36}S$, $^{18}O^{12}C^{32}S$, $^{16}O^{13}C^{34}S$, $^{18}O^{12}C^{34}S$
	$^{18}O^{13}C^{32}S$, $^{16}O^{13}C^{36}S$, $^{18}O^{12}C^{36}S$, $^{18}O^{13}C^{34}S$
H_2CS	$H_2^{12}C^{32}S$, $HD^{12}C^{32}S$, $D_2^{12}C^{32}S$, $H_2^{13}C^{32}S$
	$H_2^{12}C^{34}S$, $H_2^{12}C^{33}S$
H_2S	$H_2^{32}S$, $H_2^{36}S$, $H_2^{34}S$, $H_2^{33}S$, $DH^{32}S$, $D_2^{32}S$
HCO^+	$H^{12}C^{16}O^+$, $D^{12}C^{16}O^+$, $H^{13}C^{16}O^+$, $D^{13}C^{16}O^+$
	$H^{12}C^{18}O^+$, $D^{12}C^{18}O^+$, $H^{12}C^{17}O^+$

4. fc-CCSD(T)/CBS(5,6) + core/cc-pCVQZ + ΔT + ΔQ

5. fc-CCSD(T)/CBS(5,6) + core/cc-pCV5Z

6. fc-CCSD(T)/CBS(5,6) + core/cc-pCV5Z + ΔT

7. fc-CCSD(T)/CBS(5,6) + core/cc-pCV5Z + ΔT + ΔQ

These have been used to compute the equilibrium rotational constants, which have been compared to the semi-experimental equilibrium constants derived from the experimental B_0's by subtracting the vibrational contributions obtained at the CCSD(T)/cc-pCVQZ level.

Table II: List of molecules and isotopic species employed in the "benchmark II" study.

Molecule	Isotopologues
CS	$^{12}C^{32}S$, $^{12}C^{34}S$, $^{12}C^{33}S$, $^{12}C^{36}S$
	$^{13}C^{32}S$, $^{13}C^{33}S$, $^{13}C^{34}S$
OCS	$^{16}O^{12}C^{32}S$, $^{16}O^{13}C^{32}S$, $^{17}O^{12}C^{32}S$, $^{16}O^{12}C^{34}S$
	$^{16}O^{12}C^{36}S$, $^{18}O^{12}C^{32}S$, $^{16}O^{13}C^{34}S$, $^{18}O^{12}C^{34}S$
	$^{18}O^{13}C^{32}S$, $^{16}O^{13}C^{36}S$, $^{18}O^{12}C^{36}S$, $^{18}O^{13}C^{34}S$
H_2S	$H_2^{32}S$, $H_2^{36}S$, $H_2^{34}S$, $H_2^{33}S$, $DH^{32}S$, $D_2^{32}S$
HCl	$H^{35}Cl$, $H^{37}Cl$, $D^{35}Cl$, $D^{37}Cl$
HBS	$H^{11}B^{32}S$, $D^{11}B^{32}S$, $H^{10}B^{32}S$, $D^{10}B^{32}S$
FBS	$^{19}F^{11}B^{32}S$, $^{19}F^{11}B^{33}S$, $^{19}F^{11}B^{34}S$
	$^{19}F^{10}B^{32}S$, $^{19}F^{10}B^{33}S$, $^{19}F^{10}B^{34}S$
HCP	$H^{12}C^{31}P$, $D^{12}C^{31}P$, $H^{13}C^{31}P$, $D^{13}C^{31}P$
FCP	$^{19}F^{12}C^{31}P$, $^{19}F^{13}C^{31}P$
ClCP	$^{35}Cl^{12}C^{31}P$, $^{37}Cl^{12}C^{31}P$, $^{35}Cl^{13}C^{31}P$
SiS	$^{28}Si^{32}S$, $^{29}Si^{32}S$, $^{30}Si^{32}S$, $^{28}Si^{34}S$
PN	$^{31}P^{14}N$, $^{31}P^{15}N$

2.3 Rotational constants of sulfur containing molecules of astrochemical interest

Based the previous statistical analyses, the rotational constants for some member of the thiocumulenes family C_nS, with n=2, 3, 4 and 5 have been determined. Thiocumulenes

are linear molecules with a typical cumulene bond distance, their electronic ground state depending on the number n of carbon atoms present.[46,47] Indeed, if n is odd the molecule is a closed-shell species, while, if n is even, the molecule is an open-shell system in a $X^3\Sigma^-$ electronic ground state. Since H^+ is abundant in the ISM, the protonated species $HCCS^+$, HC_4S^+, and $HSCO^+/HOCS^+$ have also been investigated.

Due to the different computational cost required by quantum-chemical calculations, the systems under investigation have been classified in two categories:

1. "Small molecules" (CCS, $HCCS^+$, $HSCO^+$, and $HOCS^+$) with a maximum of three non-hydrogen atoms;

2. "Medium-sized molecules" (C_3S, C_4S, HC_4S^+ and C_5S) with more than three non-hydrogen atoms;

For the "small molecules" set, the best theoretical approach considered is the fc-CCSD(T)/ CBS(5,6) + core/cc-pCVQZ + ΔT + ΔQ one. For the second set consisting of the larger systems the best composite scheme to be employed is fc-CCSD(T)/CBS(T,Q) + core/cc-pCVTZ. Vibrational contributions have been considered in all cases, for the small molecules we use corrections obtained from CCSD(T)/cc-pCVQZ computations, while for the larger systems we restrict ourselves here to the fc-CCSD(T)/cc-pVTZ level of theory. In summary, the best rotational constants are obtained from the fc-CCSD(T)/CBS(5,6) + core/cc-pCVQZ + ΔT + ΔQ + ΔB_0^i(cc-pCVQZ) scheme in the case of small molecules, and with the fc-CCSD(T)/CBS(T,Q) + core/cc-pCVTZ + ΔB_0^i(cc-pVTZ) scheme for the medium-sized molecules.

Furthermore, for small systems both quartic and sextic centrifugal-distorsion constants have been determined at the CCSD(T)/cc-pCVQZ level while the electron spin-rotation constant for CCS and $HCCS^+$ are determined at the CCSD/aug-cc-pCVQZ level. The same quantities have also been computed for the "medium-sized molecules". In this case the quartic centrifugal-distortion constants have been determined at the fc-CCSD(T)/cc-pVQZ

level, while the sextic constants have been obtained at the fc-CCSD(T)/cc-pVTZ. The electron spin-rotation constants have been computed at the CCSD/aug-cc-pVTZ level for C_4S and HC_4S^+.

3 Results

3.1 Benchmark I

The rotational constants considered in the statistical analysis range from 2.7 to 310 GHz, therefore only a discussion in terms of relative errors is meaningful.[8] A summary of the experimental constants considered[48–80] is found in the Supporting Information (SI).

To analyze our results, different comparisons have been performed. First of all, a comparison between the computed B_e^i's and the equilibrium rotational constants obtained from the experimental B_0^i's by subtracting the computed vibrational corrections has been carried out. Then, to emphasize the importance of vibrational corrections a second comparison involving computed and experimental B_0^i's has been made. However, the reliability of both comparisons somewhat depend on the accuracy of vibrational corrections. For this reason, an internal theoretical comparison has also been carried out. This comparison involves the fc-CCSD(T)/CBS(Q,5) + core/cc-pCVQZ + ΔB_0^i(cc-pVTZ) results as reference. Indeed, the results obtained at the the fc-CCSD(T)/CBS(Q,5) + core/cc-pCVQZ level are close to the basis-set limit and electron-correlation effects beyond CCSD(T) can be considered small and for our purposes negligible.

Computed vs. Semi-experimental Equilibrium Rotational Constants

The results of the first comparison, i.e. those involving the semi-experimental B_e^i as reference, are reported in table III, thus showing the statistical measures for the various levels of theory considered.

Extrapolation to the CBS limit. The first contribution addressed is the convergence to the CBS limit, for which a graphical representation is provided in figure 1. It is noted that, as the basis set enlarges from cc-pVTZ to cc-pV5Z, both the mean and standard errors lower. This trend is graphically represented by tighter normal distribution functions, which are centred closer to the y-axis. However, while extrapolation to the CBS limit improves

Table III: Statistical analysis of the relative errors (in %) in the computed rotational constants with respect to B_e^i values derived from experimental B_0^i values corrected for computed vibrational contributions at the fc-CCSD(T)/cc-pVTZ level.

Computational approach	$\bar{\Delta}$	$\bar{\Delta}_{abs}$	Δ_{std}	Δ_{max}
fc-CCSD(T)/cc-pVTZ	-1.538	1.543	0.765	4.819
fc-CCSD(T)/cc-pVQZ	-0.806	0.812	0.423	2.701
fc-CCSD(T)/cc-pV5Z	-0.444	0.466	0.208	1.583
fc-CCSD(T)/CBS(T,Q)	-0.094	0.345	0.501	2.684
fc-CCSD(T)/CBS(Q,5)	-0.276	0.312	0.308	0.643
fc-CCSD(T)/cc-pV5Z+core/cc-pCVTZ	-0.118	0.183	0.192	0.787
fc-CCSD(T)/CBS(T,Q)+core/cc-pCVTZ	0.234	0.244	0.485	2.947
fc-CCSD(T)/CBS(T,Q)+core/cc-pCVQZ	0.335	0.335	0.500	3.134
fc-CCSD(T)/CBS(Q,5)+core/cc-pCVTZ	0.051	0.107	0.191	1.049
fc-CCSD(T)/CBS(Q,5)+core/cc-pCVQZ	0.151	0.160	0.188	1.199
CCSD(T)/cc-pCVQZ	-0.037	0.164	0.206	0.874

the mean error, the standard error increases with respect to the fc-CCSD(T)/cc-pV5Z level, thus resulting in broader Gaussian distributions.

Core correlation corrections. The second contribution that needs to be addressed is the effect of core correlation, with the pictorial representation given in figure 2. To understand the importance of this term, the comparison between the fc-CCSD(T)/cc-pVQZ and CCSD(T)/cc-pCVQZ levels of theory is first of all discussed. Going from the former to the latter, the standard deviation halves and the mean error decreases from -0.81% to -0.04%. Focusing the attention on additive schemes, the performance of the two core-valence basis sets used in the treatment of core correlation, namely cc-pCVTZ and cc-pCVQZ, can be analyzed. According to our statistics, when the core-correlation contribution is considered in conjunction with the extrapolation scheme, the cc-pCVTZ basis set interestingly provides slightly better mean errors, which is somewhat unexpected. However, in line with what is expected, Gaussian distributions for the fc-CCSD(T)/CBS(Q,5)+core(cc-pCVTZ) and fc-CCSD(T)/CBS(Q,5)+core(cc-pCVQZ) additive schemes appear sharper and closer to the origin with respect to the corresponding ones based on the fc-CCSD(T)/CBS(T,Q) extrapolation. This tends to suggest limitations in the extrapolation scheme using the

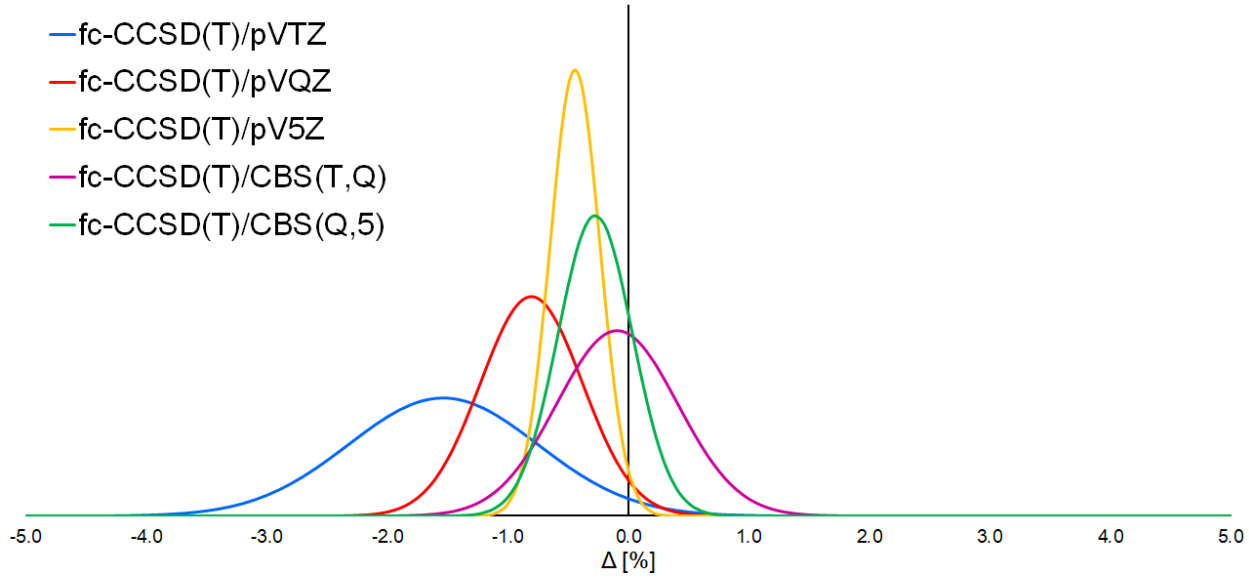

Figure 1: Comparison with semi-experimental B_e^i values: Convergence to the complete basis set limit.

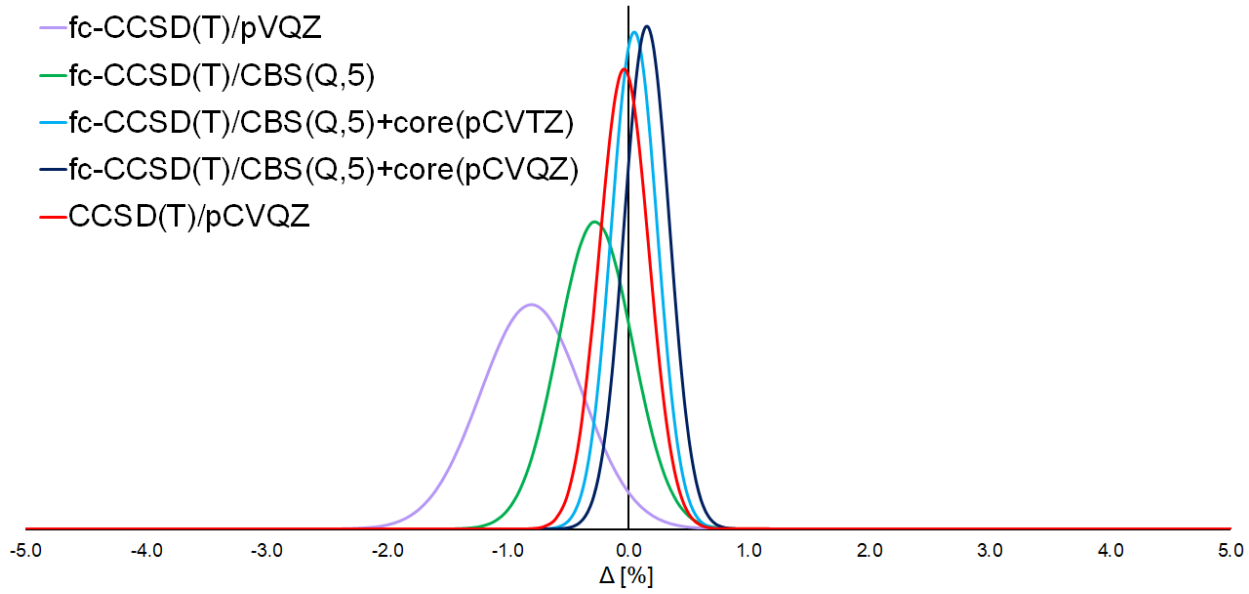

Figure 2: Comparison with experimental B_e^i values: Contribution of core correlation.

cc-pVTZ and cc-pVQZ basis sets.

Computed vs. Experimental Ground-state Rotational Constants

The previous conclusions are also confirmed by the second comparison carried out for which the statistical measures are reported in table IV (with the corresponding statistical representation given in the SI). As shown in figure 3, the fc-CCSD(T)/CBS(T,Q)-based approaches have definitely lower accuracy with respect to those based on the larger basis sets and even when vibrational corrections are added, the Δ_{std} still remains around 0.5%.

Vibrational Corrections. An important contribution to be discussed within the second comparison is the effect of vibrational corrections. Table IV points out that, even though the ΔB_0^i term accounts for a small fraction of the total B_0^i value, its inclusion is important for high accuracy. This is demonstrated by the Gaussian distributions of the fc-CCSD(T)/CBS(Q,5) + core/cc-pCVTZ + ΔB_0^i/cc-pVTZ and fc-CCSD(T)/CBS(Q,5) + core/cc-pCVQZ + ΔB_0^i/cc-pVTZ levels that are sharper than all the others, with remaining mean errors very close to zero. The former approach gives our best computed rotational constants, with a mean error of 0.06%, a standard deviation of 0.21%, and a maximum error around 1%. For the fc-CCSD(T)/CBS(T,Q) + core/cc-pCVTZ + ΔB_0^i/cc-pVTZ level, which is the theoretical approach employed for the medium-sized molecules, the standard and mean errors are 0.48% and 0.27%, respectively. In terms of absolute accuracy, to give an example, for the C_4S molecule, the computed rotational constant obtained is 1521.59 MHz and the corresponding error is expected to be 7.30 MHz.

From table IV it is noted that the fc-CCSD(T)/CBS(Q,5) + core/cc-pCVTZ + ΔB_0^i/cc-pVTZ level shows that smallest mean error, while for the standard deviation this scheme and the analogous one with core at the CCSD(T)/cc-pCVQZ level provide very similar results. The fact that the best rotational constants are not unequivocally obtained with the best theoretical approach could be due to 1) an underestimation of the vibrational corrections. 2) remaining basis-set errors in the core-correlation treatment, or 3)

missing contributions due to higher excitations in the CC treatment. To investigate the first issue, we carried out a comparison of the rotational constants obtained from the fc-CCSD(T)/CBS(T,Q) + core/cc-pCVTZ, fc-CCSD(T)/CBS(T,Q) + core/cc-pCVQZ, fc-CCSD(T)/CBS(Q,5) + core/cc-pCVTZ, and fc-CCSD(T)/CBS(Q,5) + core/cc-pCVQZ computational approaches corrected for the ΔB_0^i calculated at the fc-CCSD(T)/cc-pVTZ level and at the CCSD(T)/cc-pCVQZ. The species involved in this comparison are: SO, HCS^+, HCO^+, OCS, H_2S, CS^+, CS, and HSO, together with their corresponding isotopologues reported in table I. As shown by the results collected in table V, improved vibrational corrections do not necessarily lead to more accurate rotational constants. Indeed, only a small improvement is seen in the mean error, which is however counterpoised a slight worsening of the standard deviation. Indeed, the different performance of the fc-CCSD(T)/CBS(Q,5) + core/cc-pCVTZ + ΔB_0^i/cc-pVTZ and fc-CCSD(T)/CBS(Q,5) + core/cc-pCVQZ + ΔB_0^i/cc-pVTZ composite schemes seems to be related to the core-valence correlation treatment, with the rotational constants appearing to be slightly more overestimated when using the core-valence correlation contribution calculated with the cc-pCVQZ basis set instead of that cc-pCVTZ. However, the better performance of the CCSD(T)/cc-pCVTZ level is most likely due to error compensations between the extrapolation to the CBS limit and the core-valence contribution and/or missing ΔT and ΔQ terms.

Internal Theoretical Comparison

Moving to the third, internal comparison, we note that the fc-CCSD(T)/CBS(Q,5) + core/cc-pCVTZ level shows very similar error statistics compared to the best theoretical approach (see table VI and the corresponding graphical representation in the SI). Indeed, the standard deviation of this scheme is only 0.04% and the mean error is -0.1%. The composite scheme used for the characterization of the medium-sized molecule shows a standard deviation of 0.5% with respect to the best theoretical approach and a mean error quite small, this being 0.08%. As expected, all frozen-core results are very far from the best theoretical values and

Table IV: Statistical analysis of the relative errors (in %) in the computed rotational constants with respect to experimentally determined B_0^i values. Vibrational corrections (ΔB_0^i) computed at the fc-CCSD(T)/cc-pVTZ level.

Computational approach	$\bar{\Delta}$	$\bar{\Delta}_{abs}$	Δ_{std}	Δ_{max}
fc-CCSD(T)/cc-pVTZ	-1.252	1.349	0.913	5.184
fc-CCSD(T)/cc-pVQZ	-0.518	0.651	0.622	3.074
fc-CCSD(T)/cc-pV5Z	-0.155	0.370	0.478	2.434
fc-CCSD(T)/CBS(T,Q)	0.195	0.414	0.594	2.299
fc-CCSD(T)/CBS(Q,5)	0.013	0.339	0.575	1.705
fc-CCSD(T)/cc-pV5Z+core/cc-pCVTZ	0.172	0.346	0.459	1.941
fc-CCSD(T)/CBS(T,Q)+core/cc-pCVTZ	0.525	0.574	0.571	2.560
fc-CCSD(T)/CBS(T,Q)+core/cc-pCVQZ	0.626	0.660	0.581	2.747
fc-CCSD(T)/CBS(Q,5)+core/cc-pCVTZ	0.341	0.448	0.450	2.048
fc-CCSD(T)/CBS(Q,5)+core/cc-pCVQZ	0.442	0.502	0.449	2.040
CCSD(T)/cc-pCVQZ	0.249	0.340	0.446	2.079
fc-CCSD(T)/CBS(T,Q)+core/cc-pCVTZ + ΔB_0^i	0.261	0.244	0.485	2.936
fc-CCSD(T)/CBS(T,Q)+core/cc-pCVQZ + ΔB_0^i	0.336	0.333	0.499	3.122
fc-CCSD(T)/CBS(Q,5)+core/cc-pCVTZ + ΔB_0^i	0.055	0.113	0.194	1.053
fc-CCSD(T)/CBS(Q,5)+core/cc-pCVQZ + ΔB_0^i	0.152	0.161	0.189	1.203

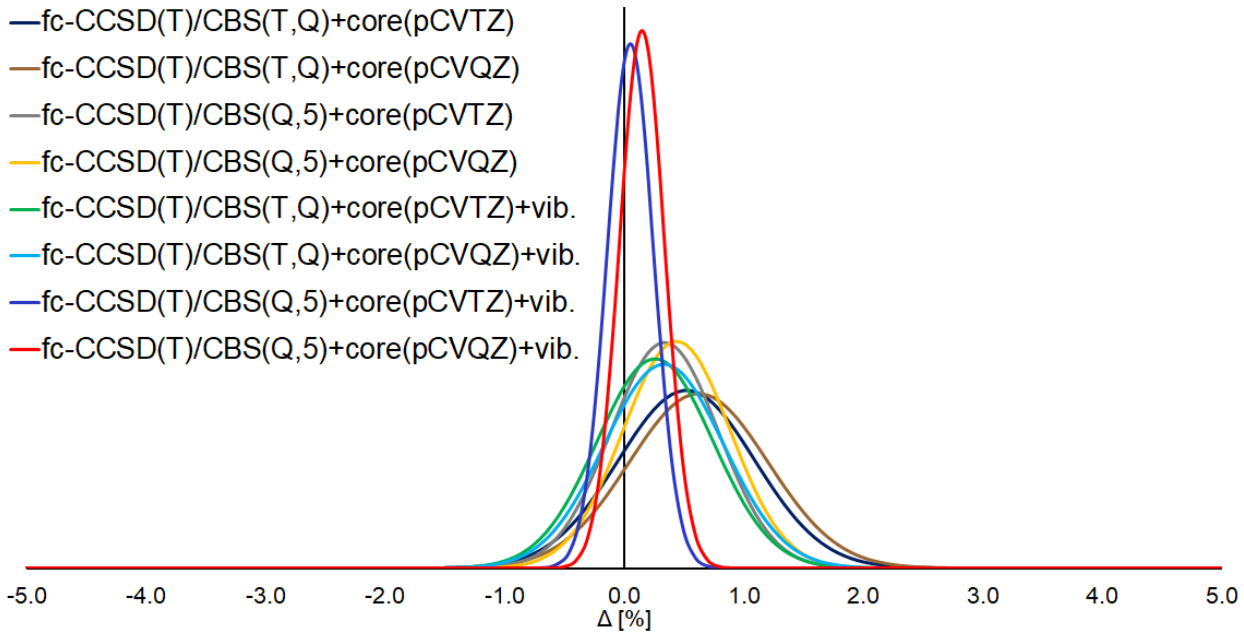

Figure 3: Comparison with experimental B_0^i values: Effect of vibrational corrections.

Table V: Comparison between the computed B_0^i values obtained using vibrational corrections at the fc-CCSD(T)/cc-pVTZ and CCSD(T)/cc-pCVQZ levels.

Computational approach	$\bar{\Delta}$	$\bar{\Delta}_{abs}$	Δ_{std}	Δ_{max}
fc-CCSD(T)/CBS(T,Q)+core/cc-pCVTZ + ΔB_0^i(cc-pVTZ)	0.190	0.192	0.287	1.173
fc-CCSD(T)/CBS(T,Q)+core/cc-pCVTZ + ΔB_0^i(cc-pCVQZ)	0.189	0.194	0.288	1.173
fc-CCSD(T)/CBS(T,Q)+core/cc-pCVQZ + ΔB_0^i(cc-pVTZ)	0.291	0.285	0.297	1.325
fc-CCSD(T)/CBS(T,Q)+core/cc-pCVQZ + ΔB_0^i(cc-pCVQZ)	0.290	0.284	0.298	1.324
fc-CCSD(T)/CBS(Q,5)+core/cc-pCVTZ + ΔB_0^i(cc-pVTZ)	0.061	0.107	0.199	1.053
fc-CCSD(T)/CBS(Q,5)+core/cc-pCVTZ + ΔB_0^i(cc-pCVQZ)	0.060	0.103	0.197	1.053
fc-CCSD(T)/CBS(Q,5)+core/cc-pCVQZ + ΔB_0^i(cc-pVTZ)	0.161	0.172	0.204	1.203
fc-CCSD(T)/CBS(Q,5)+core/cc-pCVQZ + ΔB_0^i(cc-pCVQZ)	0.160	0.173	0.207	1.203

sizeable improvements are observed only when core-correlation is considered.

Table VI: Statistical analysis of the relative errors (in %) in the computed rotational constants with respect to B_e^i values at the CCSD(T)/CBS(Q,5)+core/cc-pCVQZ level.

Computational approach	$\bar{\Delta}$	$\bar{\Delta}_{abs}$	Δ_{std}	Δ_{max}
fc-CCSD(T)/cc-pVTZ	-1.686	1.686	0.789	4.781
fc-CCSD(T)/cc-pVQZ	-0.956	0.964	0.428	2.662
fc-CCSD(T)/cc-pV5Z	-0.595	0.595	0.149	1.570
fc-CCSD(T)/CBS(T,Q)	-0.245	0.382	0.474	2.725
fc-CCSD(T)/CBS(Q,5)	-0.427	0.427	0.158	0.598
fc-CCSD(T)/cc-pV5Z+core/cc-pCVTZ	-0.269	0.272	0.128	0.529
fc-CCSD(T)/CBS(T,Q)+core/cc-pCVTZ	0.083	0.144	0.459	2.988
fc-CCSD(T)/CBS(T,Q)+core/cc-pCVQZ	0.184	0.185	0.472	3.175
fc-CCSD(T)/CBS(Q,5)+core/cc-pCVTZ	-0.100	0.100	0.038	0.336
CCSD(T)/cc-pCVQZ	-0.188	0.238	0.161	0.617

3.2 Benchmark II

In addition to investigate the role played by full triples and quadruples corrections, this benchmark study is also intended to analyze the effect of increasing the basis set from a quadruple-zeta to a quintuple-zeta in the evaluation of the core-correlation contribution. The latter is an important point because core correlation for second-row elements often needs cc-pCV5Z basis sets to be correctly taken into account. Indeed, there is some

indication in the literature that the use of a quadruple-zeta basis set is not sufficient.[57,81] As before the discussion is in term of relative errors and the experimental values used as reference[48–63,82–93] are reported in the SI.

Table VII: Statistical analysis of the relative errors (in %) in the computed rotational constants with respect to B_e^i values derived from experimental B_0^i values corrected for vibrational contribution computed at the CCSD(T)/cc-pCVQZ level.

Computational approach	$\bar{\Delta}$	$\bar{\Delta}_{abs}$	Δ_{std}	Δ_{max}
fc-CCSD(T)/CBS(5,6)	-0.406	0.406	0.112	0.774
fc-CCSD(T)/CBS(5,6) + core/cc-pCVQZ	0.057	0.077	0.101	0.369
fc-CCSD(T)/CBS(5,6) + core/cc-pCVQZ + ΔT	-0.076	0.195	0.248	0.763
fc-CCSD(T)/CBS(5,6) + core/cc-pCVQZ + ΔT + ΔQ	-0.018	0.094	0.126	0.404
fc-CCSD(T)/CBS(5,6) + core/cc-pCV5Z	0.193	0.306	0.300	0.862
fc-CCSD(T)/CBS(5,6) + core/cc-pCV5Z + ΔT	0.121	0.140	0.133	0.468
fc-CCSD(T)/CBS(5,6) + core/cc-pCV5Z + ΔT + ΔQ	0.189	0.202	0.172	0.808

The results of this benchmark are summarized in table VII. We first of all note that the apparently best results are obtained at the fc-CCSD(T)/CBS(5,6) + core/cc-pCVQZ level, with a clear worsening observed once the contribution due to full treatment of triples is included. The subsequent account of quadruple excitations lowers all statistical measures, with mean absolute error and standard deviation that are close to those at the fc-CCSD(T)/CBS(5,6) + core/cc-pCVQZ level. According to these results, the full-triples and full-quadruples give contributions that tend to cancel each other out, thus rendering their computational cost not always justified. On the other hand, in terms of the mean error the fc-CCSD(T)/CBS(5,6) + core/cc-pCVQZ + ΔT + ΔQ composite approach is the level of theory performing at best. In the case of core-correlation contributions evaluated using the cc-pCV5Z basis set, it is apparent that worse results are obtained. The large core/cc-pCV5Z correction seems to be partially balanced by the full treatment of triples, while the subsequent inclusion of the ΔQ contribution leads to a worsening. This outcome clearly deserves to be further investigated, possibly by considering a larger benchmark set. A last comment concerns relativistic and non-BO corrections. Both of them typically provide only very small contributions. For the former this is at least true for compounds

with second-row elements, for the latter this seems generally the case.[5,94,95]

3.3 Accurate prediction of rotational spectra for S-containing molecules of astrochemical interest

This section aims at discussing the results obtained for the specific sulfur-containing molecules of astronomical interest. Furthermore, general conclusions on the level of theory required for the accurate prediction of rotational spectra in the specific case of molecular species containing second-row elements are drawn.

Small-sized molecules

The results obtained for CCS, $HCCS^+$ and the protonated species of OCS are presented with particular emphasis on the accuracy obtained for each spectroscopic parameter. To discuss the accuracy of the computational schemes investigated, we have selected the CCS radical, for which the best theoretical results are reported in table VIII, where they are also compared with the best experimental data. The rotational spectrum was simulated using Pickett's SPCAT program[96] incorporated in the VMS-ROT[97] software. The agreement between the experimental B_0 and that obtained using the fc-CCSD(T)/CBS(5,6) + core/cc-pCVQZ + ΔT + ΔQ + ΔB_0^i(cc-pCVQZ) composite scheme is very good, with a relative error as small as 0.005%, which is similar to that derived in ref. 8 for molecules containing first row atoms, i.e., 0.007%. The error for the quartic centrifugal distortion constant, being around 7% at the CCSD(T)/cc-pCVQZ (all electrons) level, is rather high, but such a large error is acceptable considering the smallness of this constant. This conclusion is in line with what has been already observed in the literature (see, e.g., refs. 5,6). The theoretical value of the electronic spin-rotation interaction constant, γ, is in qualitative agreement with the experimental one with the relative error being $\sim$18%.

The theoretical data reported in table VIII have been used to simulate the rotational

Table VIII: Spectroscopic parameters of CCS. All values reported are in MHz.

Parameter	Theoretical prediction	Experimental value[77](a)
B_0	6477.403[(b)]	6477.75036(71)
D	1.6×10^{-3}[(c)]	$1.72796(95) \times 10^{-3}$
H	2.1×10^{-11}[(c)]	-
λ	97196.07[(d)]	97196.07(77)
λ_D	0.02700[(d)]	0.02700(67)
γ	-12.1[(e)]	-14.737(49)
γ_D	$5.5(37) \times 10^{-5}$[(d)]	$5.5(37) \times 10^{-5}$

[(a)] The number in parentheses represents the standard deviation in units of the last significant digits.
[(b)] fc-CCSD(T)/CBS(5,6) + core/cc-pCVQZ + ΔT + ΔQ + ΔB_0^i(cc-pCVQZ).
[(c)] CCSD(T)/cc-pCVQZ.
[(d)] Fixed to the value of Yamamoto et al..
[(e)] CCSD/aug-cc-pCVQZ.

spectrum of CCS at T=100 K (figure 4), which is compared with the experimental counterpart that has been obtained using the data from ref. 77. It can be seen that the two spectra agree quite well, with errors going from 4 MHz in the case of low frequencies up to 1 GHz for higher frequencies. In the inset of figure 4, one transition and its fine structure are shown in detail. The considered line lies at a frequency around 505 GHz and it is noted that the theoretical predictions overestimate the experimental values by $\sim$760 MHz, i.e., by about 0.15%.

To exclusively analyze the impact of the computed rotational constant on the predicted spectra, the rotational spectrum of CCS has been simulated using the B_0 constant evaluated at four different levels of theory, with all the other spectroscopic parameters fixed at the corresponding experimental values, and compared to experiment. In this way, the errors in the predicted spectra are only due to the level of theory employed for computing B_0. The computational schemes considered are: fc-CCSD(T)/CBS(5,6) + ΔB_0^i(cc-pCVQZ), fc-CCSD(T)/CBS(5,6) + core/cc-pCVQZ + ΔB_0^i(cc-pCVQZ), fc-CCSD(T)/CBS(5,6) + core/cc-pCVQZ + ΔT + ΔB_0^i(cc-pCVQZ), and fc-CCSD(T)/CBS(5,6) + core/cc-pCVQZ + ΔT + ΔQ + ΔB_0^i(cc-pCVQZ). It is noted that when only the extrapolation to the CBS limit is considered

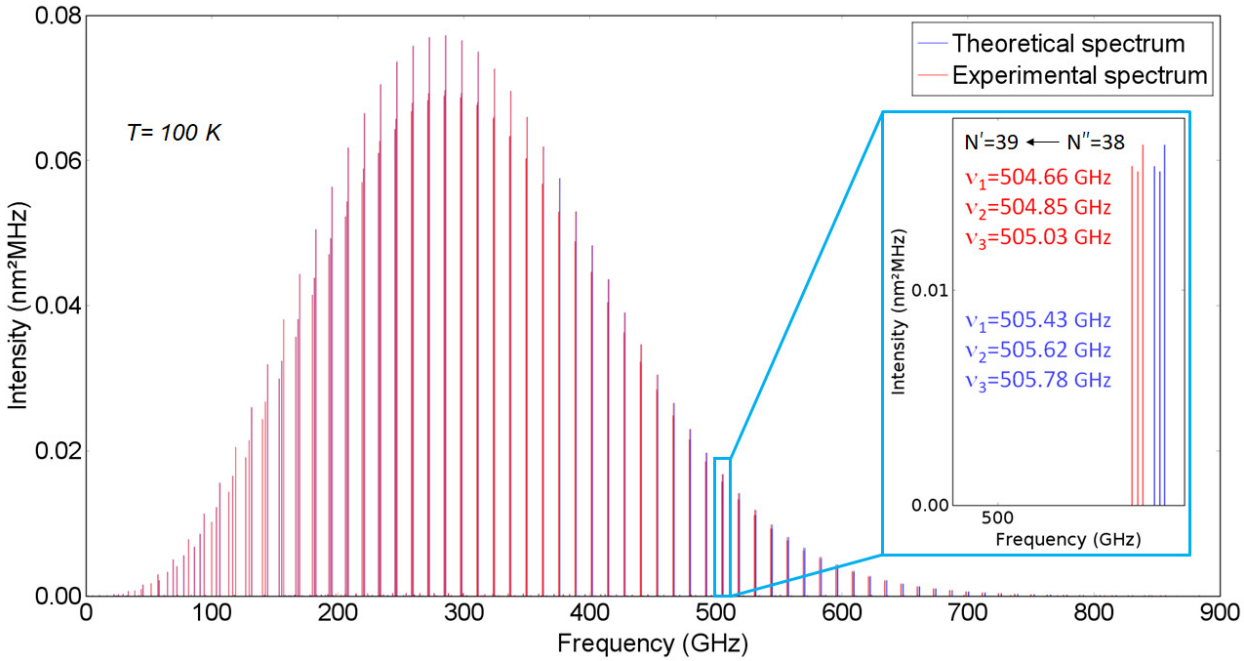

Figure 4: The rotational spectrum of CCS: comparison of experiment and theory.

the computed rotational transitions are underestimated by about 0.3%. Inclusion of the core-correlation correction leads to an overestimation by about 0.25%. The discrepancy is lowered once the full treatment of triple excitations is taken into account, with remaining deviations on the order of +0.14%. A further improvement is obtained by incorporating the effect of quadruples, thus lowering the disagreement to around -0.01%. This means that the transition frequency at ∼505 GHz is underestimated with an error of about 55 MHz. If we compare the last result with the spectrum simulated using the complete set of theoretical values VIII (see discussion in the previous paragraph), differences of about 0.16% are noted in reproducing the experimental spectrum is noted. Since in both cases the same level of theory is used for B_0, by inspecting this table, it is apparent that this discrepancy is mostly due to the limited accuracy of the computed electronic spin-rotation interaction constant γ.

A simulation of the entirely computed rotational spectrum has also been performed also for the protonated species of CCS and OCS, namely, $HCCS^+$ and $HSCO^+$, for which the experimental data present in the literature are missing or limited. A summary of the

computed spectroscopic parameters is reported in the SI and will be of future interest for experimental measurements. Indeed, the same accuracy as that obtained for CCS is expected. However, when comparing the theoretical and experimental[98] rotational constants of $HOCS^+$, larger relative errors are observed: 0.43%, 0.025% and 0.015% for the A_0, B_0, and C_0 constants, respectively. Nevertheless, these experimental data were obtained only with a very limited number of low frequency measurements and call for an improvement, and for this reason, $HOCS^+$ has not been included in the benchmark set of molecules. In particular, the accuracy of the experimental rotational constants is very limited, with a standard deviation from the fit as large as 4 MHz. Results of mixed quality have been also obtained for the quartic-centrifugal distortion constants, with errors ranging from 6 to 13%. However, once again, the experimental counterparts are not particularly accurate with one parameter (d_1) clearly wrongly determined. Furthermore, it should be noted that, as already mentioned in ref. 99, despite the fact that $HSCO^+$ is about 20 kJ/mol lower in energy than $HOCS^+$, only the latter one has been observed experimentally; this renders both protonated species worthy of further experimental investigation.

Medium-sized molecules

The discussion of the results for the medium-sized molecules is mainly focussing on the C_3S molecule. The theoretical data from the present work data are reported in table IX together with the corresponding experimental values. We note that the relative error for the rotational constant obtained at the fc-CCSD(T)/CBS(T,Q) + core/cc-pCVTZ + ΔB_0^i(cc-pVTZ) level is $\sim$0.03%, thus being nearly one order of magnitude smaller than that predicted by the benchmark study. The same trend is observed for C_5S, for which the relative error is $\sim$0.05%. Instead, for C_4S a relative error of 0.13% has been obtained. However, also this uncertainty is lower than what is expected based on the benchmark study, thus suggesting that the latter might provide rather conservative error estimates. The relative error for the quartic-centrifugal distortion constant of C_3S is around 6%, consistent

with previous results, even if the parameter has been obtained at the CCSD(T)/cc-pVQZ level of theory within the frozen-core approximation. A similar relative error is also observed in the case of C_5S, while it doubles for the C_4S radical.

As shown in figure 5, the agreement between the experimental and predicted spectra in the case of C_3S is still good. The transition highlighted in the inset indicates that deviations of ∼100 MHz are observed for frequencies above 300 GHz, i.e., deviations of about ∼0.04% in relative terms. Results of similar quality are seen for C_4S and C_5S and are expected for HC_4S^+. For all these molecules, the computational results are collected in the SI.

4 Concluding remarks

By employing different composite schemes, an accurate spectroscopic characterization has been carried out for the thiocumulenes family C_nS, with n=2, 3, 4 and 5, and for the $HCCS^+$, HC_4S^+, and $HSCO^+/HOCS^+$ protonated species. While the former family of molecules mainly allowed us to investigate the accuracy obtainable, for the cationic species accurate predictions of the rotational parameters have been provided for the first time. Different composite approaches have been investigated and their accuracy has been addressed thanks to a benchmark study. In particular, for $HCCS^+$, $HSCO^+$, and $HOCS^+$ the CCSD(T)/CBS(5,6) + core/cc-pCVQZ + ΔT + ΔQ + ΔB_0^i(cc-pCVQZ) level of theory is

Table IX: Rotational parameters of C_3S in MHz.

Parameter	Theoretical value	Experimental value[67] [(a)]
B_0	2891.27[(b)]	2890.37959(29)
D	1.96×10^{-4}[(c)]	$2.086(75) \times 10^{-4}$
H	2.00×10^{-12} [(d)]	-

[(a)] The number in parentheses represents the standard deviation in units of the last significant digits.
[(b)] fc-CCSD(T)/CBS(T,Q) + core/cc-pCVTZ + ΔB_0^i(cc-pVTZ).
[(c)] fc-CCSD(T)/cc-pVQZ.
[(d)] fc-CCSD(T)/cc-pVTZ.

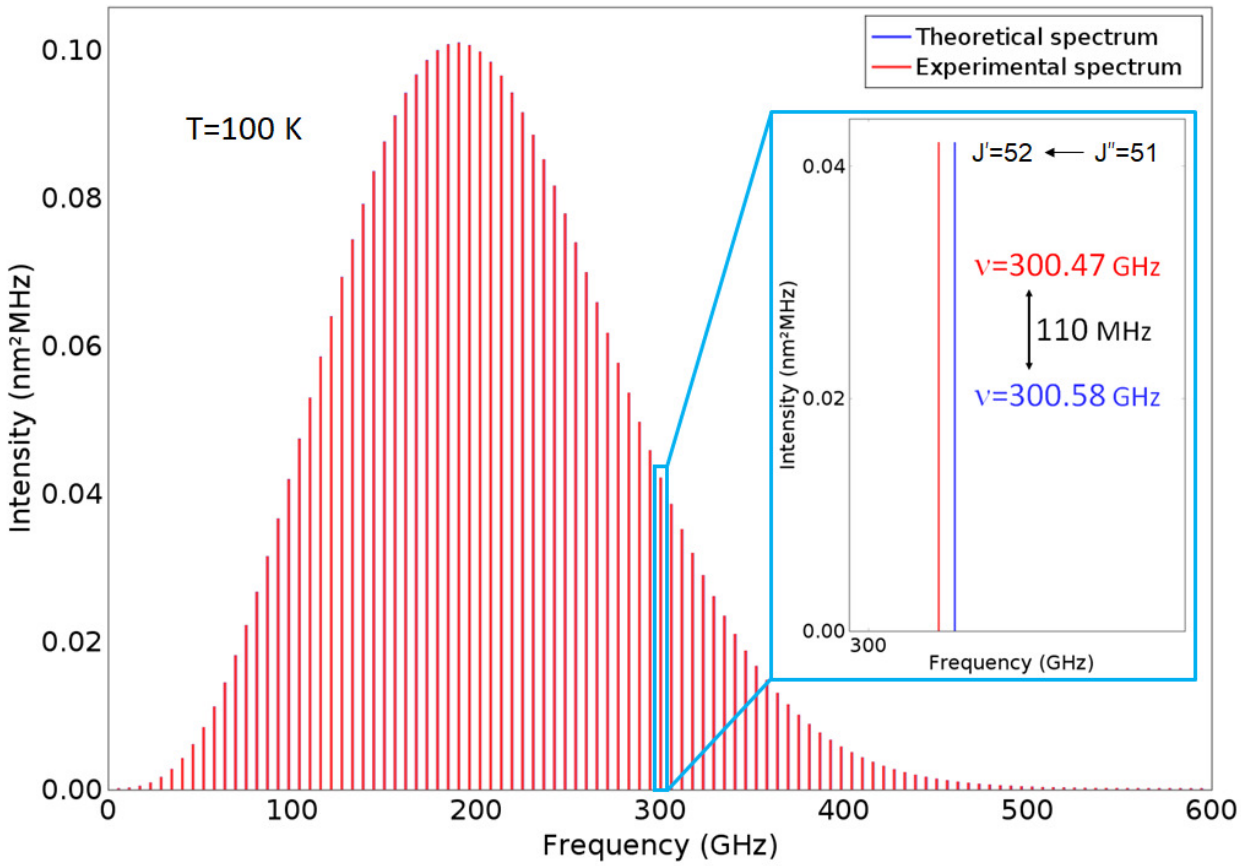

Figure 5: The rotational spectrum of C_3S: comparison of experiment and theory.

expected to provide rotational constants with an accuracy better than 0.01%. For HC_4S^+, the best approach considered is CCSD(T)/CBS(T,Q) + core/cc-pCVTZ + ΔB_0^i(cc-pVTZ), which should predict rotational constants with an accuracy better than 0.1%.

From the inspection of the results collected in Tables III and VII, it is noted that important improvements in the mean error and in the standard deviation are observed once, in conjunction with core-correlation corrections at the CCSD(T)/cc-pCVQZ level, we move from CCSD(T)/CBS(T,Q) to CCSD(T)/CBS(Q,5), and then to the CCSD(T)/CBS(5,6) extrapolation. On the other hand, according to Table V, vibrational corrections can be computed with very similar accuracy at the fc-CCSD(T)/cc-pVTZ and CCSD(T)/cc-pCVQZ levels of theory.

The optimized geometrical parameters that are at the basis of the statistical analysis reported in Table VII point out that moving from core/cc-pCVQZ to core/cc-pCV5Z leads to an additional shortening of the bond distances. This means that, once the core-correlation contribution is evaluated at the CCSD(T)/cc-pCV5Z level and coupled with extrapolation to the CBS limit performed with basis sets as large as cc-pV5Z and cc-pV6Z, the combination of the two effects ends up in bond lengths which appear to be too short, thus leading to computed rotational constants that slightly overestimate the corresponding experimental values.

Overall, the statistical analyses of the present study suggest that (*i*) the CCSD(T)/CBS(5,6) + core/cc-pCVQZ level provides high-accuracy results, not requiring full-triples and full-quadruples contributions; (*ii*) similar accuracy can be obtained only with the inclusion of the latter corrections if the extrapolation to the CBS limit is performed with smaller basis sets; (*iii*) the employment of the cc-pCV5Z basis set in the evaluation of the core-correlation contribution is discouraged unless in conjunction with CCSD(T)/CBS(Q,5); (*iv*) in the case of medium-sized molecules containing second-row elements, geometry optimizations using the CCSD(T)/CBS(T,Q) + core/cc-pCVTZ composite scheme in conjunction with vibrational corrections evaluated at the fc-CCSD(T)/cc-pVTZ level are able to provide

rotational parameters that are suitable and sufficiently accurate to guide experiment.

5 Supporting Information

The Supporting Information is available free of charge on the ACS Publications website at DOI: ...

1. Experimental values and best theoretical estimates for the rotational constants of all the isotopologues considered in the benchmark I study.

2. Experimental values for all the rotational constants considered in the benchmark II study.

3. Graphical representations of the comparison between computed and experimental rotational constants as well as of the theoretical internal comparison.

4. Computed spectroscopic parameters for $HCCS^+$, HOCS+, $HSCO^+$, C_4S, C_5S, and HC_4S^+ compared with experimental data and/or previous computational results.

6 Acknowledgments

This work has been supported in Bologna by MIUR “PRIN 2015 funds (project “STARS in the CAOS (Simulation Tools for Astrochemical Reactivity and Spectroscopy in the Cyberinfrastructure for Astrochemical Organic Species)” - Grant Number 2015F59J3R) and by the University of Bologna (RFO funds), in Mainz by the Deutsche Forschungsgemeinschaft (DFG GA 370/6-1 and 370/6-2).

References

(1) Tielens, A. G. G. M. The molecular universe. *Rev. Mod. Phys.* **2013**, *85*, 1021.

(2) Herbst, E.; Van Dishoeck, E. F. Complex organic interstellar molecules. *Annu. Rev. Astron. Astrophys.* **2009**, *47*, 427–480.

(3) Tennyson, J. *Astronomical spectroscopy: an introduction to the atomic and molecular physics of astronomical spectra*; Imperial College Press Advanced Physics Texts vol. 2; Imperial College Press, 2005.

(4) Gordy, W.; Cook, R. L. *Microwave Molecular Spectra*, 3rd ed.; Wiley, 1984.

(5) Puzzarini, C.; Stanton, J. F.; Gauss, J. Quantum-chemical calculation of spectroscopic parameters for rotational spectroscopy. *Int. Rev. Phys. Chem.* **2010**, *29*, 273–367.

(6) Puzzarini, C.; Cazzoli, G.; Gauss, J. The rotational spectra of $HD^{17}O$ and $D_2^{17}O$: experiment and quantum-chemical calculations. *J. Chem. Phys.* **2012**, *137*, 154311.

(7) Puzzarini, C. Rotational spectroscopy meets theory. *Phys. Chem. Chem. Phys.* **2013**, *15*, 6595–6607.

(8) Puzzarini, C.; Heckert, M.; Gauss, J. The accuracy of rotational constants predicted by high-level quantum-chemical calculations. I. molecules containing first-row atoms. *J. Chem. Phys.* **2008**, *128*, 194108.

(9) Puzzarini, C.; Senent, M.; Domínguez-Gómez, R.; Carvajal, M.; Hochlaf, M.; Al-Mogren, M. M. Accurate spectroscopic characterization of Ethyl mercaptan and Dimethyl sulfide isotopologues: A route toward their astrophysical detection. *Astrophys. J.* **2014**, *796*, 50.

(10) Müller, H. S.; Schlöder, F.; Stutzki, J.; Winnewisser, G. The Cologne Database for Molecular Spectroscopy, CDMS: a useful tool for astronomers and spectroscopists. *J. Mol. Struct.* **2005**, *742*, 215–227.

(11) Kolesniková, L.; Tercero, B.; Cernicharo, J.; Alonso, J.; Daly, A.; Gordon, B.; Shipman, S. Spectroscopic characterization and detection of Ethyl Mercaptan in Orion. *Astrophys. J. Lett.* **2014**, *784*, L7.

(12) Savage, B. D.; Sembach, K. R. Interstellar abundances from absorption-line observations with the Hubble Space Telescope. *Annu. Rev. Astron. Astrophys.* **1996**, *34*, 279–329.

(13) Joseph, C. L.; Snow Jr, T. P.; Seab, C. G.; Crutcher, R. M. Interstellar abundances in dense, moderately reddened lines of sight. I-Observational evidence for density-dependent depletion. *Astrophys. J.* **1986**, *309*, 771–782.

(14) Woods, P. M.; Occhiogrosso, A.; Viti, S.; Kaňuchová, Z.; Palumbo, M. E.; Price, S. D. A new study of an old sink of sulphur in hot molecular cores: the sulphur residue. *Monthly Notices of the Royal Astronomical Society* **2015**, *450*, 1256–1267.

(15) Shavitt, I.; Bartlett, R. J. *Many-body methods in chemistry and physics: MBPT and coupled-cluster theory*; Cambridge University Press, 2009.

(16) Raghavachari, K.; Trucks, G. W.; Pople, J. A.; Head-Gordon, M. A fifth-order perturbation comparison of electron correlation theories. *Chem. Phys. Lett.* **1989**, *157*, 479–483.

(17) Dunning Jr, T. H. Gaussian basis sets for use in correlated molecular calculations. I. The atoms boron through neon and hydrogen. *J. Chem. Phys.* **1989**, *90*, 1007–1023.

(18) Wilson, A. K.; van Mourik, T.; Dunning Jr, T. H. Gaussian basis sets for use in correlated molecular calculations. VI. Sextuple zeta correlation consistent basis sets for boron through neon. *J. Mol. Struct.: THEOCHEM* **1996**, *388*, 339–349.

(19) Woon, D. E.; Dunning Jr, T. H. Gaussian basis sets for use in correlated molecular

calculations. III. The atoms aluminum through argon. *J. Chem. Phys.* **1993**, *98*, 1358–1371.

(20) Stanton, J. F.; Gauss, J.; Cheng, M. L.; Harding, M. E.; Matthews, D. A.; Szalay P. G. CFOUR, a quantum chemical program package with contributions from Auer, A. A.; Bartlett, R. J.; Benedikt, U.; Berger, C.; Bernholdt, D. E.; Bomble, Y. J.; Christiansen, O.; Engel, F.; Faber, R.; Heckert, M.; Heun, O.; Huber, C.; Jagau, T.-C.; Jonsson, D.; Jusélius, J.; Klein, K.; Lauderdale, W. J.; Lipparini, F.; Metzroth, T.; Mück, L. A.; O'Neill, D. P.; Price, D. R.; Prochnow, E.; Puzzarini, C.; Ruud, K.; Schiffmann, F.; Schwalbach, W.; Simmons, C.; Stopkowicz, S.; Tajti, A.; Vázquez, J.; Wang, F.; D., W. J.; the integral packages MOLECULE (Almlöf, J. and Taylor, P. R.), PROPS (Taylor, P. R.), ABACUS (Helgaker, T.; Jensen, H. J. Aa.; Jørgensen, P.; Olsen J.) and ECP routines by Mitin, A. V. and van Wüllen, C., For the current version, see http://www.cfour.de.

(21) Noga, J.; Bartlett, R. J. The full CCSDT model for molecular electronic structure. *J. Chem. Phys.* **1987**, *86*, 7041–7050.

(22) Scuseria, G. E.; Schaefer, H. F. A new implementation of the full CCSDT model for molecular electronic structure. *Chem. Phys. Lett.* **1988**, *152*, 382–386.

(23) Kucharski, S. A.; Bartlett, R. J. The coupled-cluster single, double, triple, and quadruple excitation method. *J. Chem. Phys.* **1992**, *97*, 4282–4288.

(24) Kállay, M. MRCC, a generalized CC/CI program. For the current version, see http://www.mrcc.hu.

(25) Kroto, H. W. *Molecular rotation spectra*; Dover, 1992.

(26) Gauss, J.; Stanton, J. F. Analytic CCSD(T) second derivatives. *Chem. Phys. Lett.* **1997**, *276*, 70–77.

(27) Stanton, J. F.; Gauss, J. Analytic second derivatives in high-order many-body perturbation and coupled-cluster theories: computational considerations and applications. *Int. Rev. Phys. Chem.* **2000**, *19*, 61–95.

(28) Schneider, W.; Thiel, W. Anharmonic force fields from analytic second derivatives: Method and application to methyl bromide. *Chem. Phys. Lett.* **1989**, *157*, 367–373.

(29) Stanton, J. F.; Lopreore, C. L.; Gauss, J. The equilibrium structure and fundamental vibrational frequencies of dioxirane. *J. Chem. Phys.* **1998**, *108*, 7190–7196.

(30) Heckert, M.; Kállay, M.; Gauss, J. Molecular equilibrium geometries based on coupled-cluster calculations including quadruple excitations. *Mol. Phys.* **2005**, *103*, 2109–2115.

(31) Heckert, M.; Kállay, M.; Tew, D. P.; Klopper, W.; Gauss, J. Basis-set extrapolation techniques for the accurate calculation of molecular equilibrium geometries using coupled-cluster theory. *J. Chem. Phys.* **2006**, *125*, 044108.

(32) Feller, D. The use of systematic sequences of wave functions for estimating the complete basis set, full configuration interaction limit in water. *J. Chem. Phys.* **1993**, *98*, 7059–7071.

(33) Helgaker, T.; Klopper, W.; Koch, H.; Noga, J. Basis-set convergence of correlated calculations on water. *J. Chem. Phys.* **1997**, *106*, 9639–9646.

(34) Halkier, A.; Helgaker, T.; JÃÿrgensen, P.; Klopper, W.; Koch, H.; Olsen, J.; Wilson, A. K. Basis-set convergence in correlated calculations on Ne, N_2, and H_2O. *Chemical Physics Letters* **1998**, *286*, 243 – 252.

(35) Woon, D. E.; Dunning Jr, T. H. Gaussian basis sets for use in correlated molecular calculations. V. Core-valence basis sets for boron through neon. *J. Chem. Phys.* **1995**, *103*, 4572–4585.

(36) Peterson, K. A.; Dunning Jr, T. H. Accurate correlation consistent basis sets for molecular core–valence correlation effects: The second row atoms Al–Ar, and the first row atoms B–Ne revisited. *J. Chem. Phys.* **2002**, *117*, 10548–10560.

(37) Pawłowski, F.; Jørgensen, P.; Olsen, J.; Hegelund, F.; Helgaker, T.; Gauss, J.; Bak, K. L.; Stanton, J. F. Molecular equilibrium structures from experimental rotational constants and calculated vibration–rotation interaction constants. *The Journal of chemical physics* **2002**, *116*, 6482–6496.

(38) Tarczay, G.; Szalay, P. G.; Gauss, J. First-Principles Calculation of Electron Spin-Rotation Tensors. *J. Phys. Chem. A* **2010**, *114*, 9246–9252, PMID: 20684654.

(39) Kendall, R. A.; Dunning Jr, T. H.; Harrison, R. J. Electron affinities of the first-row atoms revisited. Systematic basis sets and wave functions. *J. Chem. Phys.* **1992**, *96*, 6796–6806.

(40) Curtiss, L. A.; Raghavachari, K.; Redfern, P. C.; Rassolov, V.; Pople, J. A. Gaussian-3 (G3) theory for molecules containing first and second-row atoms. *J. Chem. Phys.* **1998**, *109*, 7764–7776.

(41) Boese, A. D.; Oren, M.; Atasoylu, O.; Martin, J. M.; Kállay, M.; Gauss, J. W3 theory: robust computational thermochemistry in the kJ/mol accuracy range. *J. Chem. Phys.* **2004**, *120*, 4129–4141.

(42) Tajti, A.; Szalay, P. G.; Császár, A. G.; Kállay, M.; Gauss, J.; Valeev, E. F.; Flowers, B. A.; Vázquez, J.; Stanton, J. F. HEAT: High accuracy extrapolated ab initio thermochemistry. *J. Chem. Phys.* **2004**, *121*, 11599–11613.

(43) Helgaker, T.; Gauss, J.; Jørgensen, P.; Olsen, J. The prediction of molecular equilibrium structures by the standard electronic wave functions. *J. Chem. Phys.* **1997**, *106*, 6430–6440.

(44) Bak, K. L.; Gauss, J.; Jørgensen, P.; Olsen, J.; Helgaker, T.; Stanton, J. F. The accurate determination of molecular equilibrium structures. *J. Chem. Phys.* **2001**, *114*, 6548–6556.

(45) Coriani, S.; Marchesan, D.; Gauss, J.; Hättig, C.; Helgaker, T.; Jørgensen, P. The accuracy of ab initio molecular geometries for systems containing second-row atoms. *J. Chem. Phys.* **2005**, *123*, 184107.

(46) Peeso, D.; Ewing, D.; Curtis, T. A theoretical study of C_2S and C_3S. *Chem. Phys. Lett.* **1990**, *166*, 307–310.

(47) Benmensour, M. A.; Djennane-Bousmaha, S.; Boucekkine, A. DFT study of sulfur derivatives of cumulenes and their protonated forms of interstellar interest and calculations of dissociation energies of protonated forms ($SC(CH)C_{n-2}S^+$), (n=3-8). *J. Mol. Model.* **2014**, *20*, 2295.

(48) Golubiatnikov, G. Y.; Lapinov, A.; Guarnieri, A.; Knöchel, R. Precise lamb-dip measurements of millimeter and submillimeter wave rotational transitions of $^{16}O^{12}C^{32}S$. *J. Mol. Spectrosc.* **2005**, *234*, 190–194.

(49) Dubrulle, A.; Demaison, J.; Burie, J.; Boucher, D. The millimeter wave rotational spectra of carbonyl sulfide. *Z. Naturforsch. A* **1980**, *35*, 471–474.

(50) Burenin, A.; Karyakin, E.; Krupnov, A.; Shapin, S.; Val'Dov, A. Submillimeter microwave spectrum and spectroscopic constants of the OCS molecule: less abundant isotopic species of the molecule. *J. Mol. Spectrosc.* **1981**, *85*, 1–7.

(51) Kubo, K.; Furuya, T.; Saito, S. Submillimeter-wave spectrum of carbonyl sulfide: rare isotopic species. *J. Mol. Spectrosc.* **2003**, *222*, 255–262.

(52) Gottlieb, C.; Myers, P.; Thaddeus, P. Precise millimeter-wave laboratory frequencies for CS and $C^{34}S$. *Astrophys. J.* **2003**, *588*, 655.

(53) Kim, E.; Yamamoto, S. Fourier transform millimeter-wave spectroscopy of CS ($X^1\Sigma^+$) and SO ($b^1\Sigma^+$) in highly excited vibrational states. *J. Mol. Spectrosc.* **2003**, *219*, 296–304.

(54) Ahrens, V.; Winnewisser, G. Pure Rotational Spectra of CS. *Z. Naturforsch.* **1999**, *54*, 131–136.

(55) Bailleux, S.; Walters, A.; Grigorova, E.; Margulès, L. The Submillimeter-Wave Spectrum of the CS^+ Radical Ion. *Astrophys. J.* **2008**, *679*, 920.

(56) Habara, H.; Yamamoto, S.; Amano, T. Submillimeter-wave spectra of HCS and DCS. *J. Chem. Phys.* **2002**, *116*, 9232–9238.

(57) Cazzoli, G.; Lattanzi, V.; Kirsch, T.; Gauss, J.; Tercero, B.; Cernicharo, J.; Puzzarini, C. Laboratory measurements and astronomical search for the HSO radical. *Astron. Astrophys.* **2016**, *591*, A126.

(58) Habara, H.; Yamamoto, S. Microwave spectrum and molecular structure of the HSC radical. *J. Chem. Phys.* **2000**, *112*, 10905–10911.

(59) Cazzoli, G.; Puzzarini, C. The rotational spectrum of hydrogen sulfide: The $H_2^{33}S$ and $H_2^{32}S$ isotopologues revisited. *J. Mol. Spectrosc.* **2014**, *298*, 31–37.

(60) Cazzoli, G.; Puzzarini, C.; Gauss, J. Rare isotopic species of hydrogen sulfide: the rotational spectrum of $H_2{}^{36}S$. *Astron. Astrophys.* **2014**, *566*, A52.

(61) Ala'a, A.; Yurchenko, S. N.; Tennyson, J.; Martin-Drumel, M.-A.; Pirali, O. Terahertz spectroscopy of hydrogen sulfide. *J. Quantit. Spectrosc. Radiat. Transfer* **2013**, *130*, 341–351.

(62) Helminger, P.; Cook, R. L.; De Lucia, F. C. Microwave spectrum and centrifugal distortion effects of HDS. *J. Mol. Spectrosc.* **1971**, *40*, 125–136.

(63) Cook, R. L.; De Lucia, F. C.; Helminger, P. Millimeter and submillimeter wave rotational spectrum and centrifugal distortion effects of D_2S. *J. Mol. Spectrosc.* **1972**, *41*, 123–136.

(64) Maeda, A.; Medvedev, I. R.; Winnewisser, M.; De Lucia, F. C.; Herbst, E.; Müller, H. S.; Koerber, M.; Endres, C. P.; Schlemmer, S. High-frequency rotational spectrum of thioformaldehyde, H_2CS, in the ground vibrational state. *Astrophys. J. Suppl. Ser.* **2008**, *176*, 543.

(65) Marcelino, N.; Cernicharo, J.; Roueff, E.; Gerin, M.; Mauersberger, R. Deuterated thioformaldehyde in the Barnard 1 cloud. *Astrophys. J.* **2005**, *620*, 308.

(66) Cox, A. P.; Hubbard, S. D.; Kato, H. The microwave spectrum of thioformaldehyde, CD_2S, and CH_2S: Average structure, dipole moments, and ^{33}S quadrupole coupling. *J. Mol. Spectrosc.* **1982**, *93*, 196–208.

(67) Sakai, N.; Takano, S.; Sakai, T.; Shiba, S.; Sumiyoshi, Y.; Endo, Y.; Yamamoto, S. Anomalous ^{13}C Isotope Abundances in C_3S and C_4H Observed toward the Cold Interstellar Cloud, Taurus Molecular Cloud-1. *J. Phys. Chem. A* **2013**, *117*, 9831–9839.

(68) Bizzocchi, L.; Degli Esposti, C.; Dore, L. Accurate rest frequencies for the submillimetre-wave lines of C_3O in ground and vibrationally excited states below 400 cm^{-1}. *Astronom. Astrophys.* **2008**, *492*, 875–881.

(69) Brown, R. D.; Godfrey, P. D.; Elmes, P. S.; Rodler, M.; Tack, L. M. The microwave spectrum and structure of tricarbon monoxide. *J. Am. Chem. Soc.* **1985**, *107*, 4112–4115.

(70) Cazzoli, G.; Cludi, L.; Buffa, G.; Puzzarini, C. Precise THz measurements of HCO^+, N_2H^+, and CF^+ for astrophysical observations. *Astrophys. J. Suppl. Ser.* **2012**, *203*, 11.

(71) Lattanzi, V.; Walters, A.; Drouin, B. J.; Pearson, J. C. Rotational spectrum of the formyl cation, HCO^+, to 1.2 THz. *Astrophys. J.* **2007**, *662*, 771.

(72) Plummer, G.; Herbst, E.; De Lucia, F. Laboratory measurement of the J=2 to 3 rotational transition frequency of $HC^{17}O^{+}$. *Astrophys. J.* **1983**, *270*, L99.

(73) Caselli, P.; Dore, L. Laboratory and space spectroscopy of DCO^{+}. *Astron. Astrophys.* **2005**, *433*, 1145–1152.

(74) Dore, L.; Puzzarini, C.; Cazzoli, G. Millimetre-wave spectrum of $HC^{17}O^{+}$. Experimental and theoretical determination of the quadrupole coupling costant of the ^{17}O nucleus. *Can. J. Phys.* **2001**, *79*, 359.

(75) Lattanzi, V.; Cazzoli, G.; Puzzarini, C. Rare Isotopic Species of Sulfur Monoxide: The Rotational Spectrum in the THz Region. *Astrophys. J.* **2015**, *813*, 4.

(76) Margules, L.; Lewen, F.; Winnewisser, G.; Botschwina, P.; Müller, H. The rotational spectrum up to 1 THz and the molecular structure of thiomethylium, HCS^{+}. *Phys. Chem. Chem. Phys.* **2003**, *5*, 2770–2773.

(77) Yamamoto, S.; Saito, S.; Kawaguchi, K.; Chikada, Y.; Suzuki, H.; Kaifu, N.; Ishikawa, S.-I.; Ohishi, M. Rotational spectrum of the CCS radical studied by laboratory microwave spectroscopy and radio-astronomical observations. *Astrophys. J.* **1990**, *361*, 318–324.

(78) Müller, H. S.; Brünken, S. Accurate rotational spectroscopy of sulfur dioxide, SO_2, in its ground vibrational and first excited bending states, v_2= 0, 1, up to 2 THz. *J. Mol. Spectrosc.* **2005**, *232*, 213–222.

(79) Müller, H. S.; Farhoomand, J.; Cohen, E. A.; Brupbacher-Gatehouse, B.; Schäfer, M.; Bauder, A.; Winnewisser, G. The rotational spectrum of SO_2 and the determination of the hyperfine constants and nuclear magnetic shielding tensors of $^{33}SO_2$ and $SO^{17}O$. *J. Mol. Spectrosc.* **2000**, *201*, 1–8.

(80) Belov, S.; Tretyakov, M. Y.; Kozin, I.; Klisch, E.; Winnewisser, G.; Lafferty, W.; Flaud, J.-

M. High frequency transitions in the rotational spectrum of SO_2. *J. Mol. Spectrosc.* **1998**, *191*, 17–27.

(81) McCarthy, M. C.; Gauss, J. Exotic SiO_2H_2 Isomers: Theory and Experiment Working in Harmony. *J. Phys. Chem. Lett.* **2016**, *7*, 1895–1900.

(82) Cazzoli, G.; Cludi, L.; Puzzarini, C. Microwave spectrum of $P^{14}N$ and $P^{15}N$: Spectroscopic constants and molecular structure. *J. Mol. Struc.* **2006**, *780*, 260–267.

(83) Muller, H. S. P.; McCarthy, M. C.; Bizzocchi, L.; Gupta, H.; Esser, S.; Lichau, H.; Caris, M.; Lewen, F.; Hahn, J.; Degli Esposti, C.; Schlemmer, S.; Thaddeus, P. Rotational spectroscopy of the isotopic species of silicon monosulfide, SiS. *Phys. Chem. Chem. Phys.* **2007**, *9*, 1579–1586.

(84) Sanz, M. E.; McCarthy, M. C.; Thaddeus, P. Rotational transitions of SO, SiO, and SiS excited by a discharge in a supersonic molecular beam: Vibrational temperatures, Dunham coefficients, Born–Oppenheimer breakdown, and hyperfine structure. *J. Chem. Phys.* **2003**, *119*, 11715–11727.

(85) Bizzocchi, L.; Degli Esposti, C.; Dore, L. Sub-Doppler millimetre-wave spectroscopy of DBS and HBS: accurate values of nuclear electric and magnetic hyperfine structure constants. *Phys. Chem. Chem. Phys.* **2008**, *10*, 658–665.

(86) Cazzoli, G.; Puzzarini, C. Hyperfine structure of the J=1 $\leftarrow$ 0 transition of $H^{35}Cl$ and $H^{37}Cl$: improved ground state parameters. *J. Mol. Spectrosc.* **2004**, *226*, 161–168.

(87) Cazzoli, G.; Puzzarini, C. Hyperfine structure of the J = 1 $\leftarrow$ 0 and J = 2 $\leftarrow$ 1 transitions of $D^{35}Cl$ and $D^{37}Cl$. *Phys. Chem. Chem. Phys.* **2004**, *6*, 5133–5139.

(88) Bizzocchi, L.; Degli Esposti, C.; Dore, L.; Puzzarini, C. Lamb-dip millimeter-wave spectroscopy of HCP: Experimental and theoretical determination of ^{31}P nuclear

spin–rotation coupling constant and magnetic shielding. *Chem. Phys. Lett.* **2005**, *408*, 13–18.

(89) Dréan, P.; Demaison, J.; Poteau, L.; Denis, J.-M. Rotational Spectrum and Structure of HCP. *J. Mol. Spectrosc.* **1996**, *176*, 139–145.

(90) Bizzocchi, L.; Thorwirth, S.; Müller, H. S.; Lewen, F.; Winnewisser, G. Submillimeter-wave spectroscopy of phosphaalkynes: HCCCP, NCCP, HCP, and DCP. *J. Mol. Spectrosc.* **2001**, *205*, 110–116.

(91) Bizzocchi, L.; Degli Esposti, C.; Puzzarini, C. Millimetre-wave spectroscopy and ab initio calculations for fluorophosphaethyne (FCP). *Mol. Phys.* **2006**, *104*, 2627–2640.

(92) McNaughton, D.; Bruget, D. The infrared spectrum of chlorophosphaethyne, ClCP. *J. Mol. Spectrpsc.* **1993**, *161*, 336–350.

(93) Bizzocchi, L.; Esposti, C. D. Pyrolysis of sulfur tetrafluoride over boron: Excited-state rotational spectra and equilibrium structure of fluorothioborine (FBS). *J. Chem. Phys.* **2001**, *115*, 7041–7050.

(94) Puzzarini, C.; Cazzoli, G.; Gauss, J. Rotational spectra of isotopic species of silyl fluoride. Part II: Theoretical and semi-experimental equilibrium structure. *J. Mol. Spectrosc.* **2010**, *262*, 37–41.

(95) Gauss, J.; Puzzarini, C. Quantum-chemical calculation of Born-Oppenheimer breakdown parameters to rotational constants. *Mol. Phys.* **2010**, *108*, 269–277.

(96) Pickett, H. M. The fitting and prediction of vibration-rotation spectra with spin interactions. *J. Mol. Spectrosc.* **1991**, *148*, 371 – 377.

(97) Licari, D.; Tasinato, N.; Spada, L.; Puzzarini, C.; Barone, V. VMS-ROT: A New Module of the Virtual Multifrequency Spectrometer for Simulation, Interpretation, and Fitting of Rotational Spectra. *J. Chem. Theory Comput.* **2017**, *13*, 4382–4396.

(98) Nakanaga, T.; Amano, T. High-resolution infrared identification of $HOCS^+$ with difference frequency laser spectroscopy. *Mol. Phys.* **1987**, *61*, 313–323.

(99) Taylor, P. R.; Scarlett, M. The rotational spectra of $HOCO^+$, $HOCS^+$, $HSCO^+$, and $HSCS^+$. *Astrophys. J.* **1985**, *293*, L49–L51.